Egyptian Journal of Aquatic Biology & Fisheries
Zoology Department, Faculty of Science,
Ain Shams University, Cairo, Egypt.
ISSN 1110 – 6131
Vol. 27(4): 707 – 727 (2023)
www.ejabf.journals.ekb.eg

Carbon Sequestration in mangrove sediments as Climate Change Mitigation Tool: A Case Study from the Red Sea, Egypt

Asmaa Awad[1], Amr El-Sammak[1], Ahmed Elshazly[1&2] and Esraa A. El-Masry[1*]
[1] Department of Oceanography, Faculty of Science, Alexandria University, Alexandria, Egypt
[2] Heliopolis University for Sustainable Development, Cairo, Egypt
[*]**Corresponding Author:** esraaelmasry@alexu.edu.eg

ARTICLE INFO
Article History:
Received: May 27, 2023
Accepted: July 17, 2023
Online: Aug. 11, 2023

Keywords:
Mangroves,
Sediment organic carbon,
Carbon sequestration potential,
Red Sea,
Climate Change mitigation,
Carbon credit.

ABSTRACT

Blue carbon ecosystems such as mangroves consider a significant carbon pool through their ability to store carbon dioxide from the atmosphere in their sediments and biomass for long periods. Two areas along the Red Sea coast of Egypt were selected for this study (Wadi El Gemal and Hamata areas). The aim of the present study is to understand the capacity of mangroves to store carbon through these objectives: (1) quantify carbon sequestration potential (CSP), (2) detect the mangrove areas change using Geographic Information System (GIS). Results indicated that all mangrove short cores showed an increasing trend of SOC content with depth. The (SOC) contents reach the maximum value at deeper layers with an average of 7.59 ±6.13 g C_{org} kg^{-1}. The estimated capacity of the carbon pools in mangrove sediments in the Wadi El Gemal area was 5.39 ±0.59 kg C_{org} m^{-2} while in the Hamata area, it was 2.25 ±0.19 kg C_{org} m^{-2}. The mean carbon sequestration rate (CSR) in mangrove sediments in the Wadi El Gemal area was 81.87 ±7.1 g C_{org} m^{-2} yr^{-1} while in the Hamata area was 34.24 ±2.9 g C_{org} m^{-2} yr^{-1}. Mangroves in Egypt can mitigate CO2 emissions with a value ranging from 0.0478 to 0.1145 Mt ha-1, equivalent to the total carbon price that fluctuated from 0.9168 to 2.195 MUS$. The total area of mangroves in the study area showed an increase in the area from 56810 m^2 in 2001 to 64710 m^2 in 2021. The mangrove extent area's net gain reached 7900 m^2 from 2001 to 2021 due to plantation projects. Protecting and managing mangrove areas offer enormous economic benefits for carbon stock and mitigation of climate change.

1. INTRODUCTION

Climate change is a serious phenomenon, which is one of the most significant challenges facing human beings in the 21^{st} century. It causes by human activities that increase Green House Gases (GHG) concentration; hence many consequences can be observed such as an increase in the average global temperature, sea level rise, climate-related extreme events, heatwaves, droughts, floods, cyclones, wildfires, significant alternation of some ecosystems and disruption of food production and water supply **(IPCC, 2014)**. One of the main contributors to climate change is CO_2. One of the mechanisms to reduce CO_2 concentrations is to support CO_2 uptake and storage in natural ecosystems with high C sequestration rates **(McLeod *et al.*, 2011)**.

Blue Carbon (BC) is the organic carbon that is taken and kept by the oceans and coastal ecosystems, such as vegetated coastal ecosystems, mangrove forests, tidal marshes, and seagrass meadows. These coastal ecosystems constitute hotspots of carbon cycling and are among the most oversized carbon sinks in the biosphere, as a result, the contrivance of the term "BC" in 2009 was the growing recognition of the potential quantitative significance of marine ecosystems in climate change mitigation **(Geraldi *et al.*, 2019; Jennerjahn, 2021)**.

Furthermore, these ecosystems serve as important transitional habitats, providing essential ecosystem services to both marine and terrestrial organisms **(Radabaugh *et al.*, 2018)**.

Mangrove forests consist of tropical trees and woody shrub plants growing in the intertidal zone of tropical and subtropical regions and are highly productive ecosystems, covering about 137,760 km^2 worldwide in 118 countries and territories **(Giri *et al.*, 2011)**. Globally, mangrove forests comprise approximately fifty-four species from twenty different families of vascular plants **(Hernández and Junca-Gómez, 2020)**.

Mangroves are considered major ecosystems in the carbon cycle and storage along tropical and subtropical coastlines. As a result, potentially up to 98% of their carbon content is stored in their sediments, and organic matter can accumulate over several meters in depth on decades to millennial time scales **(Jacotot *et al.*, 2018)**.

Climate change affects mangroves and their sedimentary carbon deposits by influencing a wide range of processes at various spatial and temporal scales. Mangrove's vulnerability to climate change is determined by its exposure, sensitivity, and adaptive capacity **(Ward *et al.*, 2016; Lovelock and Reef, 2020)**. With the implementation of good management practices, legislation, and clear frameworks for ownership and use, current trends in mangrove loss can be significantly slowed. The right economic settings and incentives for improved management and conservation will only be created if the true value of mangroves is recognized**.**

The carbon credit is a marketable certificate that allows the holder to emit one ton of CO_2 or a comparable amount of any greenhouse gas. The principal goal of establishing carbon credits is to reduce CO_2 and other greenhouse gas emissions to mitigate climate change’s effects **(Gupta, 2011)**. Carbon credit offers a mitigation tool for reducing GHG emissions. Several studies find that carbon price is more effective in reducing emissions and a more cost-effective solution for mitigating climate change

(Estrada *et al.*, 2015). Mangroves could become a carbon trading market if carbon credits are used **(Hong *et al.*, 2017)**.

In Egypt mangrove stands are dispersed along the Egyptian Red Sea coastline in sheltered bays and lagoons protected behind coral reefs. The mangrove stands in Egypt cover a total area exceeding 525 hectares **(Shaltout *et al.*, 2019)**. They are predominantly mono-specific, consisting only of *Avicennia marina* (*A. marina*), except a few stands in the southern Sudanese border area where *Rhizophora mucronata* (*R. mucronata*) coexists along with *A. marina*. This explains *A. marina* is relatively more tolerant and adapted to salinity, low rainfall, and extreme temperature conditions than *R. mucronata*. Result in larger global and local distribution of *A. marina* than *R. mucronate* **(Afefe *et al.*, 2019)**.

The evaluation of the carbon sequestration capacity of mangroves along Red Sea has been discussed by few authors **(Eid *et al.*, 2016; Almahasheer *et al.*, 2017; Arshad *et al.*, 2018; Cusack *et al.*, 2018; Eid *et al.*, 2020; Shaltout *et al.*, 2020)**. Few studies have been carried out the organic carbon in mangrove sediments along Red Sea of Egypt **(Ahmed and Khedr, 2007; Madkour e*t al.*, 2014; Eid and Shaltout, 2016; El-Hussieny and Ismail, 2017; Afefe *et al.*, 2019; Afefe *et al.*, 2020; El Hussieny *et al.*, 2021)**. The mapping of mangrove areas along Red Sea has been discussed by few authors **(Saleh, 2007; Almahasheer *et al.*, 2016; Abd-El Monsef *et al.*, 2017; Khawfany *et al.*, 2017; Abdel-Hamid *et al.*, 2018; Basheer *et al.*, 2019)**.

Carbon sequestration and mapping of mangrove areas in the Red Sea of Egypt did not receive much attention in the recent research. It is critical to establish a baseline for carbon sequestration potential in the mangrove of the Red Sea coast sediments as well as estimating the area of mangroves. The present study aims to assess carbon sequestration capacity in the sediments of selected mangrove areas along the Red Sea Coast of Egypt, in relation to Climate Change through evaluating of Sediment Organic Carbon Density (SOC_D) and Sediment organic carbon pool (SOC_P), estimating of Carbon Sequestration Rate (CSR) and Carbon Sequestration Potential (CSP) of selected the mangrove areas, valuation of mangrove as mitigation measure for Climate Changes will be estimated using the most common carbon emission price, and evaluating the state and trend of mangroves distribution in the study area using GIS techniques.

2. STUDY AREA

The Red Sea Coast of Egypt extends about 1200 km from Suez (Lat. 29° 58′N, Long. 32° 32′E) to Marsa Halaib (Lat. 22° 14′N, Long. 36° 39′E) at the Sudanese-Egyptian border. The surface water salinity varies from 36.5 ‰ in the south to 40.5 ‰ in the north **(Eid and Shaltout, 2016; Shaltout *et al.*, 2019)**. Geomorphologically, the coastal zone of the Red Sea on the Egyptian side is generally narrow. The beach varies from rocky to sandy, with low or high relief topography of cliffs and headlands. Mostly, the beach is backed by a wide coastal plain followed by rocky mountains belonging to the Eastern Desert **(Abd El wahab, 2010)**. Recently, there are some man-made modifications in many parts of the Red **(Abd El wahab, 2010)**. The coastal area is also characterized by manifestations of aesthetic ecosystems and natural habitats represented in coastal lagoons, salt marshes, mudflats, sand dunes, beaches, mangrove trees, and coral reefs extending along the coast **(Azab *et al.*, 2020)**.

Sampling was carried out during January 2021 at two stations along the southern Egyptian Red Sea coast. St.1 represents mangrove in Wadi El Gemal area and St.2 represent mangrove in Hamata area (St.1: 24^{o} 18’ 27” N, 35^{o} 21’ 44” E; St.2: 24^{o} 22’ 44” N, 35^{o} 15’ 50” E) (Figure 1). The two sites were chosen based local knowledge indicating the healthy nature of the mangroves at both sites. The mangroves at Wadi El Gemal and Hamata is healthy and dense where trees can reach heights up to 5.5 m. The current study focused on the mangrove species *A. marina* stands spread over a large area along a coastal zone with mud flats.

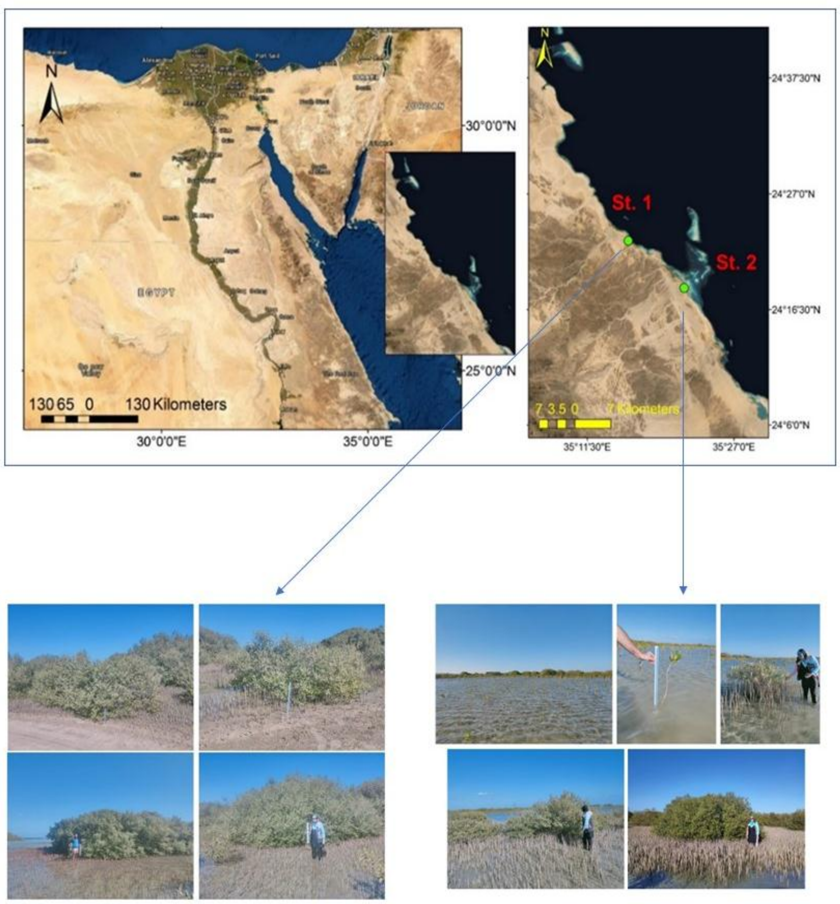

Figure (1): Map of sampling sites: St.1 Wadi El Gemal area, St.2 Hamata area.

3. MATERIALS AND METHODS

3.1 Field work

Sediments were collected using PVC cores of 60 cm length and 7 cm internal diameter from the Wadi El Gemal and Hamata areas. Two cores were collected from each site, one core was collected from the mangrove area, while the other core was collected from sandy area and is used as reference area. The samples of mangrove sediments were expressed as M1, M2 and R1, R2 for the mangroves and reference cores at Wadi El Gemal area and Hamata area, respectively. Cores were manually hammered into the sediment until resistance prevented further percussion. The sediment core was immediately sectioned with a blade into 8 samples each of 5 cm length and packed in plastic containers. The sample containers were tightly sealed and stored in frozen box to avoid volatilization losses and to minimize microbial activity until analysis **(Eid and Shaltout, 2016)**.

3.2 Sediment parameters determination

Total carbonates were determined in the samples using the method described by **Madkour and Mohammed (2008)**. The sediment bulk density was determined following the method described by Wilke (2005); Sediment Bulk Density was calculated by using the following equations

$$\rho b = M / V$$

Where ρb bulk density (g/cm^3), M mass of the core sample dried at 105 °C, V volume of the core sample (cm^3).

Sediment Organic Carbon (OC) was measured using "Carbon and sulfur analyzer BK-CSA5". (Table 1) illustrates the equations used for calculations of the blue carbon parameters.

Table 1. Equations of calculating sediment parameters

Parameter	Equation	Reference
1. Sediment organic carbon density	$SOC_{Dj} = \rho b_i \times SOC_i$	**(Han *et al.*, 2010)**
2. Sediment organic carbon pool	$SOC_p = \frac{\sum_{i=1}^{n} SOC_{Di} * T_i}{\sum_{i=1}^{n} T_i} * D_r$	**(Meersmans *et al.*, 2008)**
3. Carbon sequestration rate	$CSR_i = \rho b_i * SOC_i * R$	**(Xiaonan *et al.*, 2008)** **(El-Hussieny and Ismail, 2017)**
4. Carbon sequestration potential	$CSP = CSR_i * A$	**(Xiaonan *et al.*, 2008)**

Where:

- SOC_{Di} = sediment organic carbon density (kg C_{org} m^{-3}) of the i th layer
- ρb_j = the Sediment bulk density (g cm^{-3}) of the i th layer,
- SOC_i = the Sediment organic carbon content (g C_{org} kg^{-1}) of the i th layer)
- SOC_p = sediment organic carbon pool (kg C_{org} m^{-2}),
- T_j= thickness of the i^{th} horizon (m), n= number of horizons, and D_r= reference depth (m)
- CSR_i is carbon sequestration rate (g C_{org} m^{-2} $year^{-1}$) of the i^{th} layer (mangroves area), R= sedimentation rate in the Red Sea
- CSP = carbon sequestration potential (Gg Corg year-1) of mangrove stands
- A = area (m^2) of mangrove stands

Statistical analyses were achieved using SPSS Ver. 25 (SPSS 2017). All the data were statistically treated to estimate the relation between sediment parameters. Graphical representation is used to show the differences between the mangrove and reference sediments in Wadi El Gemal and Hamata areas as well as the vertical variation with each core.

3.3 Carbon dioxide equivalent

The carbon dioxide equivalent was calculated using the following equation:

$$CO_2\,e\ (T\ ha^{-1}) = \text{carbon stock}\ (T\ ha^{-1}) \times 3.67$$ **(Hong *et al.*, 2017)**.

The average "Carbon Market Price" proposed by **Hong *et al.* (2017)** was used for calculating economic benefits of carbon storage. The average carbon price is 19.18 USD $ in the regulated market for every ton of CO_2 e.

3.4 Remote Sensing and GIS

Remote Sensing and GIS technique was used to assess the mangrove area coverage along the shoreline of the Red Sea of Egypt. The data were collected using high-resolution satellite images from (2001-2021) (Table 2).

Table 2. Selected information of the acquired Landsat dataset

Year	Name of Satellite/Sensor	Path/Row	Date (dd/mm/y)	Spatial resolution (m)
2001	Landsat 5 (TM)	173/36	28/07/2001	30
2021	Landsat 8 (OLI8)	173/36	03/07/2021	30

The Normalized Difference Vegetation Index (NDVI) in combination with the visual interpretation approach was used **(Nguyen *et al.*, 2020)**. The study determined the threshold values of NDVI for each land cover type (mangrove forests, water bodies, and others). This was used to construct a thematic land cover map each year with the support of the ground reference data. NDVI was calculated using the following formula.

NDVI= (Band NIR-Band RED)/ (BandNIR+BandRED)**(Rousel *et al.*, 1973; Green *et al.*, 1998).**

Where Band NIR is a near-infrared band, and Band RED is a red band Near-infrared color. Accuracy assessments were conducted by comparing the classification results with reference data that was thought to reflect accurately true land covers **(Dan *et al.*, 2016)**.

4. RESULTS AND DISCUSSION

4.1 Charactrisitcs of the sediments

The mean sediment grain size (M_z) is within the sand size. It ranged between 2.13 ϕ (fine sand) to 3.28 ϕ (very fine sand) with an average 2.61 ±0.52 ϕ (fine sand), and from 2.12 ϕ (fine sand) to 2.95 ϕ (fine sand) with an average 2.63 ±0.27ϕ (fine sand) for M1 and R1, respectively. The M_z in mangrove sediments for site 2 ranged from 1.1 ϕ (medium sand) to 2.65 ϕ (fine sand) with an average 1.89 ±0.62 ϕ (medium sand), and from 1.03 ϕ (medium sand) to 2.3 ϕ (fine sand) with an average 1.64 ±0.52 ϕ (medium sand) for the S2 and R2 respectively. The vertical distribution of mean grain size indicates that there is a decrease grain size with depth as well as similarity in M_z profiles for the sediments from mangrove sites (M1 and M2) value with depth, (Figure 2). However, the profiles of grain size changes with depth for mangrove sediments (M1, and M2) as well as those from reference areas (R1 and R2). On the other hand, there is a general increase in the sorting values with depth, hence sorting become more poorly sorted with depth (Figure 2).

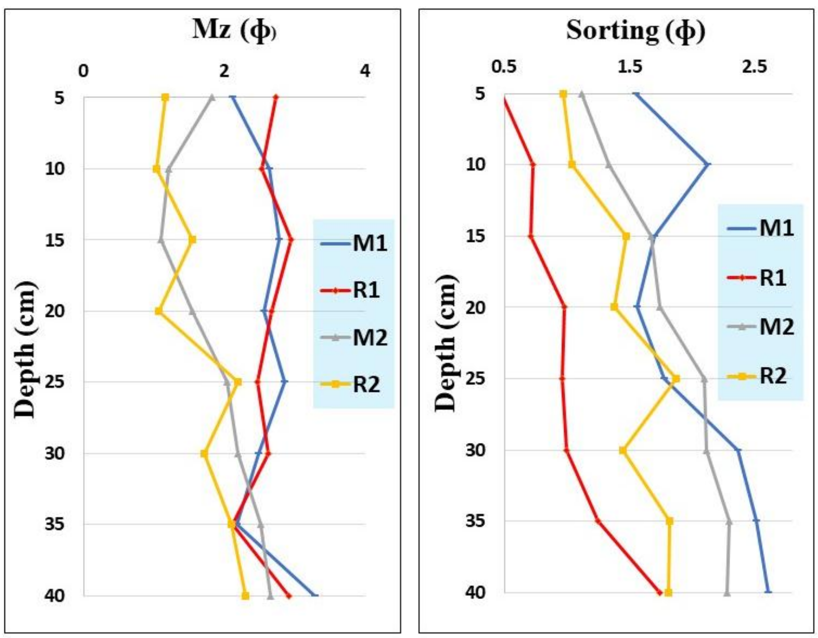

Figure (2): Distribution of Mean grain Size (M_z) and sorting (ϕ) with depth.

The variations of total carbonates contents (TCO_3%) and Sediment Bulk Density (SBD) with depth represented in Figure 3 . In general, TCO_3 contents in mangrove sediments represent less than 20% of the total sediment contents. The SBD ranged within a narrow range (1.44 g cm^{-3} to 1.57 g cm^{-3} and 1.12 g cm^{-3} and 1.62 g cm^{-3} for M2 for M1 and M2, respectively). In general SBD varies within narrow range for both mangrove and reference sediment samples.

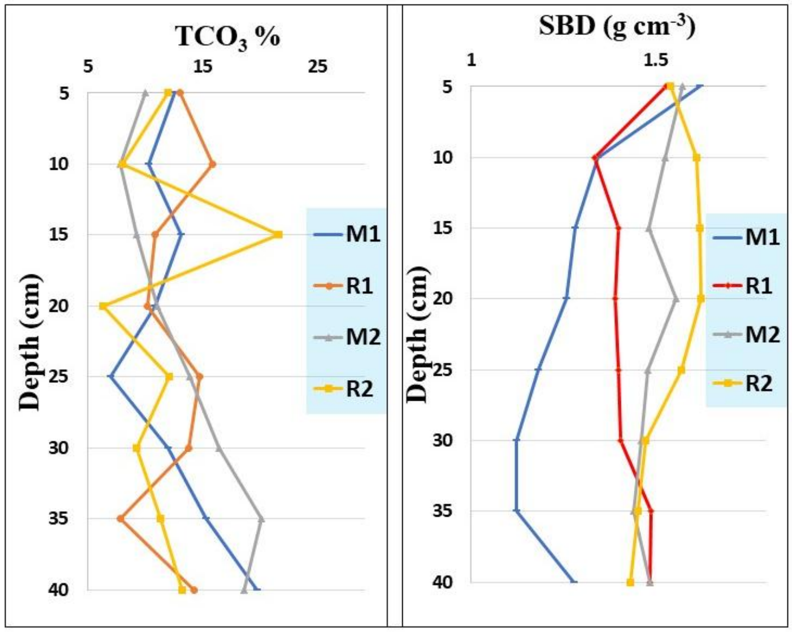

Figure (3): Distribution of TCO_3 (%) and SBD (g cm^{-3}) with depth.

4.2 Carbon content in the sediments

St.1 has the highest Sediment organic carbon (SOC) content (3.95 g C_{org} kg^{-1} in surface layers, 29.05 g C_{org} kg^{-1} in deeper layers with an average of 11.34 $\pm$9.84 g C_{org} kg^{-1}), while in St.2 SOC content range (1.05 g C_{org} kg^{-1} in surface layers, 8.19 g C_{org} kg^{-1} in deeper layers with average 3.83 $\pm$2.41 g C_{org} kg^{-1}). The general trend is that the deeper layer (35-40 cm) contained higher carbon contents than the surface layers 5-10 cm (Figure 4). Contrary to the mangrove areas, SOC contents for the reference areas vary within narrow range (The values ranged between 1.53 g C_{org} kg^{-1} and 2.61 g C_{org} kg^{-1} with an average of 2.08 $\pm$0.39 g C_{org} kg^{-1}, while in St.2 SOC was 0.71 g C_{org} kg^{-1} to 1.29 g C_{org} kg^{-1} average 0.89 $\pm$0.24 g C_{org} kg^{-1}). In general, reference sediments have lowest SOC content compare with sediment collected from mangrove sites. Consequently, the capacity of mangrove sediments to store carbon is significant. These results are similar to values observed for similar mangrove area along the Red Sea coast of Egypt, where the higher SOC content was recorded in mangrove sediments **(Eid and Shaltout, 2016)**. Similar observations were reported from mangrove surface sediments of the southern coast of Egypt's Red Sea **(Ahmed and Khedr, 2007; Madkour *et al.*, 2014; Afefe *et al.*, 2019)**. These results are compatible with studies in arid regions according to **(Almahasheer *et al.*, 2017; Chatting e*t al.*, 2020)**. Globally, SOC content is less than the results mentioned by **Castillo *et al.* (2017)**.

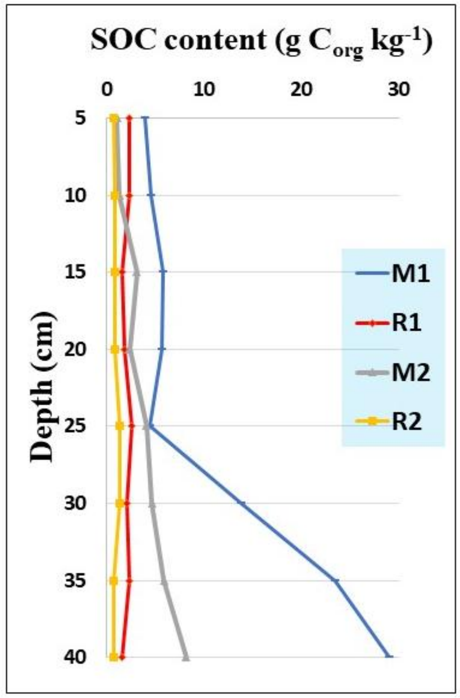

Figure (4): Distribution of SOC content (g C_{org} kg^{-1}) with depth.

The sudden increase in SOC content at M1 with a depth of 30-40 cm could be due to several factors where the sediments of M1 having the finest grain size and lowest sorting values, particularly at deeper layers (30-40 cm). Sediment porosity increase with increasing soring, hence will allow the organic carbon migration from surface layers to deeper layers. On the other hand, this area has extensive roots which support the fixation of organic carbon in deeper layers. In addition to that the SBD values are lowest at depths of 30-40 cm, and there is an inverse relationship between organic carbon and SBD.

The values of SOC content in mangrove and reference sediments in the Wadi El Gemal and Hamata areas are shown in Table (3) below. Despite M1 having the highest SOC content than M2, the ratio of increase from top to the bottom of organic carbon storage was the same. The higher values in M1 are due to the extensive trees in the Wadi El Gemal area.

Sediment organic carbon density (SOC_D) values are significant carbon reserve with a range of 1.65 kg C_{org} cm^{-3} to 36.45 kg C_{org} cm^{-3} in mangrove sediments of the studied areas. The values registered in reference sediments varied from 1.02 kg C_{org} cm^{-3} to 3.66 kg C_{org} cm^{3}. The change of SOC_D with depth in different cores in St.1 indicates that in mangrove sediments minimum SOC_D was 5.28 kg C_{org} m^{-3} at depth 25 cm and the maximum was 36.45 g C_{org} kg^{-1} at depth 40 cm with an average of 13.47 ± 11.99 kg C_{org} m^{-3} and in reference sediments, the minimum was 2.13 kg C_{org} m^{-3} at depth 15 cm and the maximum was 3.66 kg C_{org} m^{-3} at depth 25 cm with average 2.97 ± 0.57 kg C_{org} m^{-3}.

While the change of SOC_D with depth in St.2 varied in mangrove sediments between 1.65 kg C_{org} m^{-3} at depth 5 cm to 12.12 kg C_{org} m^{-3} at depth 40 cm with average 5.62 $\pm$3.88kg C_{org} m^{-3} and in reference sediments, the minimum and maximum SOC_D was 1.02 kg C_{org} m^{-3} at depth 40 cm to 2.02 kg C_{org} m^{-3} at depth 25 cm with average 1.38 $\pm$0.38kg C_{org} m^{-3} (Figure 5). Obviously, Wadi El Gemal area has values of SOC_D higher than those recorded in Hamata area, these values are compatible with the observations SOC_D (11.7 kg C_{org} m^{-3}) recorded by **El Hussieny *et al.* (2021)** in western Red Sea coast of Egypt. Values of SOC_D in southern Saudi Arabian along the Red Sea coast were four times as high as that evaluated in this study which was (SOC_D equal 42.4 kg C_{org} m^{-3}) **(Eid and Shaltout, 2016).**

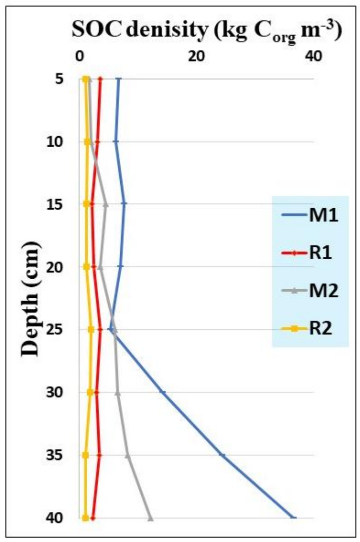

Figure (5): Distribution of SOC density (kg C_{org} m^{-3}) with depth.

Table 3. Sediment organic carbon content (g C_{org} kg^{-1}) reserved in mangrove and reference sediments at depths ranging from 5 to 40 cm at the two study areas.

Depth \ Area	Wadi El Gemal		Hamata	
	M1	**R1**	**M2**	**R2**
5 cm	3.95	2.33	1.05	0.74
10 cm	4.53	2.32	1.33	0.85
15 cm	5.79	1.53	3.11	0.79
20 cm	5.71	1.82	2.33	0.78
25 cm	4.46	2.61	4.09	1.29
30 cm	13.77	2.1	4.64	1.28
35 cm	23.49	2.29	5.89	0.72
40 cm	29.05	1.59	8.19	0.71
Average ±SD	**11.34±9.84**	**2.08 ±0.39**	**3.83±2.41**	**0.89 ±0.24**

Table 4. illustrates the results of correlation analysis. The positive correlation between Mz and SOC content confirms the fact that organic carbon is always associated with fine sediments. The SOC content and SOC density have positive correlations with depth and TCO_3%. Inversely, SBD shows negative relation with SOC content, SOC density and depth.

Table 4. The correlation among variables Mz (ϕ), TCO_3%, SBD (g cm^{-3}), SOC content (g C_{org} kg^{-1}), SOC density (kg C_{org} m^{-3}), and depth (cm).

		Correlations					
		Depth	**Mz**	**SOC content**	**SBD**	**SOC density**	**TCO_3**
Depth	**Correlation**	1	.385*	.404*	-.340*	.403*	.341*
	Sig.		.015	.011	.028	.011	.028
Mz	**Correlation**	.385*	1	.389*	-.595**	.412**	.386*
	Sig.	.015		.014	.000	.010	.015
SOC content	**Correlation**	.404*	.389*	1	-.625**	.990**	.410**
	Sig.	.011	.014		.000	.000	.010
SBD	**Correlation**	-.340*	-.595**	-.625**	1	-.566**	-.093
	Sig.	.028	.000	.000		.000	.306
SOC density	**Correlation**	.403*	.412**	.990**	-.566**	1	.448**
	Sig.	.011	.010	.000	.000		.005
TCO3%	**Correlation**	.341*	.386*	.410**	-.093	.448**	1
	Sig.	.028	.015	.010	.306	.005	

*. Correlation is significant at the 0.05 level.
**. Correlation is significant at the 0.01 level.

4.3 Carbon storage and sequestration

The values of sediment organic carbon pool (SOC_P) in mangrove sediments of the studied areas were 5.39 ±0.59 kg C_{org} m^{-2} in St.1 and 2.25 ±0.19 kg C_{org} m^{-2} in St.2. The values of reference sediments ranged between 1.19 ±0.03 kg C_{org} m^{-2} in St.1 and 0.55 ±0.02 kg C_{org} m^{-2} in St.2 (Table 5). The values of SOC_P explain the ability of mangrove sediments to retain more carbon per unit area than reference sediments. The results of SOC_P are less than assessed for other areas in the Red Sea of Egypt (Eid and Shaltout, 2016) and in Red Sea of Saudi Arabia **(Arshad *et al.*, 2018),** but the values of the present study are more than the values that mentioned in **Eid *et al.* (2016)**. On a global scale, these results are less than mentioned in **Perera and Amarasinghe (2019).**

The average carbon sequestration rate (CSR) in mangrove sediments was 81.87 ±7.05 g C_{org} m^{-2} yr^{-1} in St.1, while in St.2 was 34.24 ±2.9 g C_{org} m^{-2} yr^{-1}. Compared with reference sediments was 17.79 ±1.5 g C_{org} m^{-2} yr^{-1} St.1, while in St.2 was 8.28 ±0.7 g C_{org} m^{-2} yr^{-1} (Table 5). The carbon CSR of mangrove sediments in Wadi El Gemal area is twice that in Hamata area and is more than the reference sediments which suggests the ability of mangroves to store more carbon per unit area per year than the unvegetated sediments. In comparison with other studies, the present results are higher than those from the Gebel Elba protected area along the Red Sea, Egypt which was 13.81 g C_{org} m^{-2} yr^{-1} **(Afefe *et al.*, 2020)**, and **(Cusack *et al.*, 2018)** where CSR value in mangrove sediments is 19 g C_{org} m^{-2} yr^{-1}. These results are lower than the mean value of CSR reported for mangroves globally 163 g C_{org} m^{-2} yr^{-1} **(Breithaupt *et al.*, 2012)**.

Table 5. Mean SOC_P and CSR in mangrove and reference sediments at the two study areas.

Area	Key	SOC_P (kg C_{org} m^{-2})	CSR (g C_{org} m^{-2} yr^{-1})
Wadi El Gemal	M1	5.39 ±0.59	81.87 ±7.1
	R1	1.19 ±0.03	17.79 ±1.5
Hamata	M2	2.25 ±0.19	34.24 ±2.9
	R2	0.55 ±0.02	8.28 ±0.7

The carbon sequestration potential (CSP) values differ among mangrove sediments (Table 6). These values are more than the values mentioned by **El-Hussieny and Ismail (2017)** along the Red Sea of Egypt. The results of CSP along the Eastern Red Sea are compatible with the present study **(Shaltout *et al.*, 2020)** and less than mentioned in **Eid *et al.* (2016)**. In the present study, the average organic carbon reserved in mangrove sediments is more than the global mean mentioned in **Howard *et al.* (2017)**.

Table 6. Mean CSP in mangrove sediments at different cores at the two study areas.

Area	CSP (Gg C_{org} yr^{-1})	Reference
Wadi El Gemal, Egypt	0.43 ±0.03	Present study
Hamata, Egypt	0.18 ±0.02	Present study
Gulf of Aqaba, Egypt	0.12	**(El-Hussieny and Ismail, 2017)**
southern Saudi Arabian Red Sea coast	0.27	**(Shaltout *et al.*, 2020)**
Red Sea coast, Saudi Arabia	3.47	**(Eid *et al.*, 2016)**
Global scale	0.03	**(Howard *et al.*, 2017)**

4.4 Carbon dioxide equivalent and carbon market price

Egypt's CO_2 emissions in 2005 were 167.6 Mt CO_2 e **(EEAA, 2016)**. Mangroves in Egypt mitigate CO_2 emissions by a range 0.0478 to 0.1145 Mt ha^{-1} for the total mangroves area. Obviously, the total carbon dioxide equivalent to the studied areas was 154.53 T ha^{-1} where Wadi El Gemal area represents 218.03 T ha^{-1} and for

Hamata area it was 91.02 T ha^{-1} (Table 7). This variation is due to the Hamata area has newly planted mangroves, while Wadi El Gemal area has natural mangroves. The total economic valuation of carbon stock in the studied areas was 5,927.57 US$, (4,181.81 US$ for Wadi El Gemal area and 1,745.76 US$ in the Hamata area) (Table 7). The total carbon price of the total area of mangroves in Egypt fluctuated from 0.9168 to 2.195 MUS$. These results reflect the importance of protecting and managing natural mangrove areas for the enormous economic benefit of carbon stock and for mitigation of the climate change.

Table 7. Estimated CO_2 e (t ha^{-1}) and the carbon price of carbon stock (US$) in the studied areas.

Area	Wadi El Gemal	Hamata
CO_2 e (T ha^{-1})	218.03	91.02
A carbon price of carbon stock (US$)	4,181.812	1,745.76

4.5 Mangrove determination by using GIS and RS

Mangroves are considered a unique type of forest although it is occupying only 0.4% of global forests **(Wang *et al.*, 2019)**. Mangrove area in Egypt about 5.25 km^2 for the interval 2004 – 2020 **(Madkour and Mohammed, 2008; Salem *et al.*, 2008; Madkour *et al.*, 2014; Eid and Shaltout, 2016; Basheer *et al.*, 2019; Shaltout *et al.*, 2019; Afefe *et al.*, 2020)**.

Mangroves in Egypt's the Red Sea have been exposed to intense human activity for several years ago, such as coastal development, Irresponsible tourism activities, pollution, and accumulation of solid waste along the coast. Other issues that affect mangroves include camel grazing, woodcutting for wood and charcoal, and plant diseases **(Afefe, 2021)**. All these factors are causing mangrove loss across Egypt's Red Sea. Hence, Egypt's national project to expand mangrove forests along the coast of the Red Sea is meant to improve the environmental conditions, address climate change risks and achieve economic gains. Egypt will plant 210 hectares of mangrove trees along the Red Sea coast in Hamata, Safaga and Shalateen areas as well as Nabq Nature Reserve in South Sinai Province. Four plant nurseries were established to cultivate 50,000 seedlings every year, adding 300,000 mangrove trees.

The Wadi El Gemal and Hamata areas were estimated at 0.05681 km^2 in 2001, while in 2021 the areas were 0.06471 km^2 (Figure 6). Along with that observed significant mangrove increase across the sites between 2001 and 2021. Mangroves area increased over the years due to the plantation projects such as those in the Hamata area. The remaining mangrove areas are at risk and need protection, rehabilitation actions.

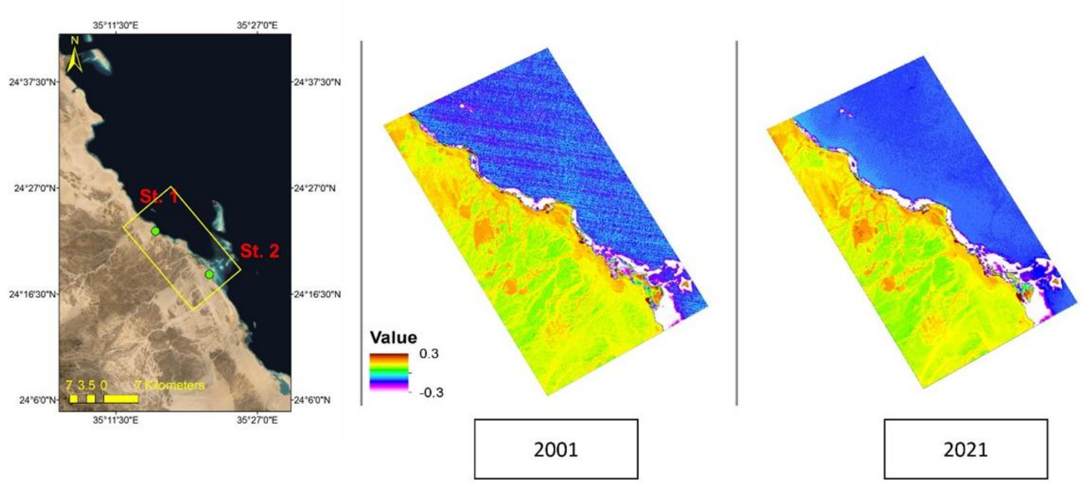

Figure (6): NDVI for years 2001 and 2021.

Clearly, the results of this study showed that the mangrove sediments in the Wadi El Gemal area have a higher level of carbon sequestration than those in the Hamata area. The results demonstrated that SOC content patterns in the areas of the study illustrated a strong positive correlation with depth and there is a strong correlation between SOC content and Mz. The Hamata area contains a large area of mangrove plantations, indicating that planted mangroves that cannot store as much carbon as natural mangroves. The results showed that the average carbon sequestration potential is less than the global mean may be due to several reasons, the harsh environmental conditions, the oligotrophic nature, as well as the lack of rivers supplying sediments to these mangrove stands **(Almahasheer *et al.*, 2017)**. Mangrove heights in the studied areas are small and not dense reflecting the impacts of climate change **(Cusack *et al.*, 2018)**. In general, climate change considers the ultimate anthropogenic disturbance factor on mangroves resulting in a maximum loss of 10 – 15% of mangrove ecosystems globally **(Taylor and Stephenson, 2017).** Sea-level rise (SLR) poses one of the greatest and most widely researched threats to coastal ecosystems like mangroves globally **(Taylor and Stephenson, 2017)**. Changes in SLR can cause sediment erosion, inundation stress, and increased salinity in mangrove habitats. According to **Dewidar (2011)** the Shoreline of Marsa Alam and Hamata areas has changed as a result of climate change which negatively impacts mangroves in these areas. Sequentially, SLR as well as lack of rainfall can threaten mangrove environments that leading to reducing the geographic area where mangroves grow. Mangroves are among the most efficient carbon sinks worldwide, but they are considered the most threatened and rapidly disappearing natural habitats **(Eid and Shaltout, 2016)**. According to **Afefe (2021)** the following impacts will pose major threats to mangrove forests along the Egyptian Red Sea coast; pollution from solid waste along the coast, woodcutting for wood and charcoal, camel grazing, plant diseases, and irresponsible tourism such as human trampling, and disturbance. Over the last years, one-third of the world's mangroves have been lost, making them one of the most endangered ecosystems that need protection **(Alongi, 2002)**. Mangroves require protection by establishing management action and administrative capacity for the mangrove ecosystems through strengthening the effectiveness of mangrove ecosystem protection, rehabilitation, and development. Promoting sustainable management of the mangrove ecosystem in response to climate change and mitigating its effects by reinforcing conservation and protection measures of mangroves, while ensuring their social and economic benefits of it **(Afefe, 2021)**.

The global rate of mangrove loss is 3-5 times, with over a quarter of the original mangrove cover already lost, so it is crucial to protect mangrove habitats. The protection of mangroves must meet the need for socio-economic development by maintaining the values and biodiversity of mangroves. The distribution of mangroves is critical for conservation efforts and further mangrove research **(Wang *et al.*, 2019)**. The conservation of mangroves could be through many initiatives 1- protected areas which are a significant policy tool for global habitat protection and recovery, and they can help to prevent further mangrove loss and degradation. 2- Promote sustainable use of mangroves and reduce mangrove conversion and degradation by reducing stressors such as development, exploitation, and pollution. 3- Mangrove restoration. 4- Involving local communities, indigenous people, and relevant economic sectors that benefit from mangroves, is critical to the success of mangrove conservation and restoration projects. 5- National policies and multilateral environmental agreements relating to mangroves. 6- Financial incentives could help to maintain ecosystem service provision **(Romañach *et al.*, 2018; Afefe, 2021)**.

5. CONCLUSION

The mangrove sediments are the main carbon sinks in the studied area and other several publications and studies. The distribution of SOC content was higher seven times in the mangrove sediments than in the reference sediments. Within the studied areas the carbon sequestration in mangrove sediments in the Wadi El Gemal area is two times more than that Hamata area along the Red Sea of Egypt. Clearly, the potential of mangroves in carbon sequestration has a significant role in developing climate change mitigation. The results of carbon sequestration in mangrove sediments of the Red Sea of Egypt differentiated from other mangrove sediments worldwide, because of several reasons the oligotrophic nature of the Red Sea, the planted mangroves do not store carbon as natural mangroves, and the destruction and degradation of the mangrove ecosystem. The deterioration of mangroves could be caused by anthropogenic activities such as land-use changes and climate change impacts, which are significant causes of mangrove degradation and the depletion of sediment organic carbon pools.

REFERENCES

Abd-El Monsef, H., ; Hassan, M.A.A. and Shata, S. (2017). Using spatial data analysis for delineating existing mangroves stands and siting suitable locations for mangroves plantation. Comput. Electron. Agric., 141: 310 – 326. https://doi.org/10.1016/j. compag.2017.08.002.

Abd El wahab, M. (2010). Overview on the effect of tourism development on the coastal zone of Red Sea, Egypt. Egypt. J. Aquat. Res., 36(2): 263 – 275.

Abdel-Hamid, A.; Dubovyk, O.; El-Magd, I. and Menz, G. (2018). Mapping Mangroves Extents on the Red Sea Coastline in Egypt using Polarimetric SAR and High Resolution Optical Remote Sensing Data. Sustainability., 10 (3): 646 – 668 . https://doi.org/10.3390/su10030646.

Afefe, A. (2021). Linking Territorial and Coastal Planning: Conservation Status and Management of Mangrove Ecosystem at the Egyptian - African Red Sea Coast. Aswan Univ. J. Environ. Stud., 2(2): 91 – 114. https://doi.org/10. 21608/aujes.2021.65951.1013.

Afefe, A.; Abbas, M.; Soliman, A.; Khedr, A.H. and Hatab, B. (2020). Tree biomass and soil carbon stocks of a mangrove ecosystem on the Egyptian-African Red Sea coast. Fund. Appl. Limnol., 193: 239 – 251. https://doi.org/10. 1127/fal/2020/1240.

Afefe, A.A.; Abbas, M.S.; Soliman, A.S.; Khedr, A.H. and Hatab, E.E. (2019). Physical and chemical characteristics of mangrove soil under marine influence. A case study on the Mangrove Forests at Egyptian-African Red Sea Coast. Egypt. J. Aquat. Biol. Fish., 23(3): 385 – 399. https://doi.org/10.21608/ ejabf. 2019.47451.

Ahmed, E.K. and Khedr, A. (2007). Zonation Pattern of Avicennia marina and Rhizophora mucronata along the Red Sea Coast, Egypt. World Appl. Sci. J., 2: 283 – 288.

Almahasheer, H.; Aljowair, A.; Duarte, C. and Irigoien, X. (2016). Decadal Stability of Red Sea Mangroves. Estuar. Coast. Shelf Sci., 169: 164 – 172. https://doi.org/10.1016/j.ecss.2015.11.027.

Almahasheer, H.; Serrano, O., Duarte; C.M.; Arias-Ortiz, A.; Masque, P. and Irigoien, X. (2017). Low Carbon sink capacity of Red Sea mangroves. Sci. Rep., 7(1),: 9700 – 9709 . https://doi.org/10.1038/s41598-017-10424-9.

Alongi, D. (2002). Present State and Future of the World's Mangrove Forests. Environ. Conserv., 29, 331– 349. https://doi.org/10.1017/S0376892902000231.

Arshad, M.; Alrumman, S. and Eid, E. (2018). Evaluation of carbon sequestration in the sediment of polluted and non-polluted locations of mangroves. Fund. Appl. Limnol., 192: 53 – 64. https://doi.org/10.1127/fal/2018/1127.

Azab, A.; El-Khadragy, A.A. and Saada, S.A. (2020). A new contribution to the geology of the Egyptian Red Sea shelf using geophysical data. Geophys. Prospect. 68(5): 1575 –1612. https://doi.org/10.1111/1365-2478.12939.

Basheer, M.; Kafrawy, S. and Mekawey, A. (2019). Identification of mangrove plant using hyperspectral remote sensing data along the Red Sea, Egypt. Egypt. J. Aquat. Biol. Fish., 33(1): 27 – 36. https://doi.org/10.21608/ejabf.2019.25932.

Breithaupt, J.L.; Smoak, J.M.; Smith Iii, T.J.; Sanders, C.J. and Hoare, A. (2012). Organic carbon burial rates in mangrove sediments: Strengthening the global budget. Global Biogeochem. Cycles., 26(3): GB3011. https://doi.org/ https://doi.org/10.1029/2012GB004375.

Castillo, J.A.A.; Apan, A.A.; Maraseni, T.N., and Salmo, S.G. (2017). Soil C quantities of mangrove forests, their competing land uses, and their spatial distribution in the coast of Honda Bay, Philippines. Geoderma., 293: 82 – 90. https://doi.org/10.1016/j.geoderma.2017.01.025.

Chatting, M.; LeVay, L.; Walton, M.; Skov, M.W.; Kennedy, H.; Wilson, S. and Al-Maslamani, I. (2020). Mangrove carbon stocks and biomass partitioning in an extreme environment. Estuar. Coast. Shelf Sci., 244: 106940. https://doi.org/10.1016/j.ecss.2020.106940.

Cusack, M.; Saderne, V.; Arias-Ortiz, A.; Masqué, P.; Krishnakumar, P.; Rabaoui, L.; Qurban, M.; Qasem, A.; Prihartato, P.; Loughland, R.; Elyas, A. and Duarte, C. (2018). Organic carbon sequestration and storage in vegetated coastal habitats along the western coast of the Arabian Gulf. Environ. Res. Lett., 13(7): 1–10. https://doi.org/10.1088/1748-9326/aac899.

Dan, T.T.; Chen, C.F.; Chiang, S.H. and Ogawa, S. (2016). Mapping and change analysis in mangrove forest. ISPRS Ann. Photogramm. Remote Sens. Spatial Inf. Sci., III-8: 109 – 116. https://doi.org/10.5194/isprs-annals-III-8-109-2016.

Dewidar, K. (2011). Changes in the Shoreline Position Caused by Natural Processes for Coastline of Marsa Alam - Hamata, Red Sea, Egypt. Int. J. Geosci., 2: 523 – 529. https://doi.org/10.4236/ijg.2011.24055.

Eid, E. and Shaltout, K., (2016). Distribution of soil organic carbon in the mangrove Avicennia marina (Forssk.) Vierh. along the Egyptian Red Sea Coast. Reg. Stud. Mar. Sci., 3: 76 – 82. https://doi.org/10.1016/j.rsma.2015.05.006.

Eid, E.M.; El-Bebany, A.F. and Alrumman, S.A. (2016). Distribution of soil organic carbon in the mangrove forests along the southern Saudi Arabian Red Sea coast. Rend. Lincei., 27(4): 629 – 637. https://doi.org/10.1007/s12210-016-0542-6.

Eid, E.M.; Khedher, K.M.; Ayed, H.; Arshad, M.; Moatamed, A. and Mouldi, A. (2020). Evaluation of carbon stock in the sediment of two mangrove species, Avicennia marina and Rhizophora mucronata, growing in the Farasan Islands, Saudi Arabia. Oceanologia., 62(2): 200 – 213. https://doi.org/10.1016/j.oceano.2019.12.001.

El-Hussieny, S.A. and Ismail, I.M. (2017). Role of Avicennia marina (Forssk.) Vierh. of South Sinai, Egypt in Atmospheric CO2 Sequestration. Int. J. Sci. Res., 6: 1935 –1943. https://doi.org/10.21275/ART20171097.

El Hussieny, S.A.; Shaltout, K.H. and Alatar, A.A. (2021). Carbon sequestration potential of Avicennia marina (Forssk.) Vierh. and Rhizophora mucronata Lam. along the Western Red Sea Coast of Egypt. Rend. Lincei., 32(3): 599 – 607. https://doi.org/10.1007/s12210-021-01005-0.

Estrada, G.; Soares, M.; Cavalcanti, V. and Almeida, P.M. (2015). The economic evaluation of carbon storage and sequestration as ecosystem services of mangroves: A case study from southeastern Brazil. Int. J. Biodivers. Sci. Ecosyst. Serv. Manag., 11: 29 – 35. https://doi.org/10.1080/21513732.2014.963676.

Geraldi, N.R.; Ortega, A.; Serrano, O.; Macreadie, P.I.; Lovelock, C.E.; Krause-Jensen, D.; Kennedy, H.; Lavery, P.S.; Pace, M.L.; Kaal, J. and Duarte, C.M. (2019). Fingerprinting Blue Carbon: Rationale and Tools to Determine the Source of Organic Carbon in Marine Depositional Environments. Front. Mar. Sci., 6: 1 – 9. https://doi.org/10.3389/fmars.2019.00263.

Giri, C.; Ochieng, E.; Tieszen, L.L.; Zhu, Z.; Singh, A.; Loveland, T.; Masek, J. and Duke, N. (2011). Status and distribution of mangrove forests of the world using earth observation satellite data. Glob. Ecol. Biogeogr., 20(1): 154 – 159. https://doi.org/10.1111/j.1466-8238.2010.00584.x.

Green, E.P.; Clark, C.D.; Mumby, P.J.; Edwards, A.J. and Ellis, A.C. (1998). Remote sensing techniques for mangrove mapping. Int. J. Remote Sens., 19(5): 935 – 956. https://doi.org/10.1080/014311698215801.

Gupta, M. Y. (2011). Carbon credit: a step towards green environment. Glob. J. Manag. Bus. Res., 11(5): 1 – 5.

Han, F.; Hu, W.; Zheng, J.; Du, F. and Zhang, X. (2010). Estimating soil organic carbon storage and distribution in a catchment of Loess Plateau, China. Geoderma., 154(3): 261 – 266. https://doi.org/10.1016/j.geoderma.2009.10.011.

Hernández, M.E. and Junca-Gómez, D. (2020). Carbon stocks and greenhouse gas emissions (CH4 and N2O) in mangroves with different vegetation assemblies in the central coastal plain of Veracruz Mexico. Sci. Total Environ., 741: 140276. https://doi.org/10.1016/j.scitotenv.2020.140276.

Hong, L.; Hemati, Z. and Zakaria, R. (2017). Carbon Stock Evaluation of Selected Mangrove Forests in Peninsular Malaysia and its Potential Market Value. J. Environ. Sci. Manag., 20: 77 – 87. https://doi.org/10.47125/jesam/2017_2/09.

Howard, J.; Sutton-Grier, A.; Herr, D.; Kleypas, J.; Landis, E.; McLeod, E.; Pidgeon, E. and Simpson, S. (2017). Clarifying the role of coastal and marine systems in climate mitigation. Front. Ecol. Environ., 15(1): 42 – 50. https://doi.org/10.1002/fee.1451.

IPCC (2014). Climate Change Impacts, Adaptation, and Vulnerability. Part A: Global and Sectoral Aspects. Contribution of Working Group II to the Fifth Assessment Report of the Intergovernmental Panel on Climate Change. Summary for policymakers, in: Field, C.B.; Barros, V.R.; Dokken, D.J.; Mach, K.J.; Mastrandrea, M.D.; Bilir, T.E.; Chatterjee, M.; Ebi, K.L.; Estrada, Y.O.; Genova, R.C.; Girma, B.; Kissel, E.S.; Levy, A.N.; MacCracken, S.; Mastrandrea, P.R. and White, L.L. (Eds.), Cambridge University Press, Cambridge. pp. 1-32.

Jacotot, A.; Marchand, C.; Rosenheim, B.E.; Domack, E.W. and Allenbach, M. (2018). Mangrove sediment carbon stocks along an elevation gradient: Influence of the late Holocene marine regression (New Caledonia). Mar. Geol., 404: 60 – 70. https://doi.org/10.1016/j.margeo.2018.07.005.

Jennerjahn, T.C. (2021). Relevance and magnitude of 'Blue Carbon' storage in mangrove sediments: Carbon accumulation rates vs. stocks, sources vs. sinks. Estuar. Coast. Shelf Sci., 248: 107156. https://doi.org/10.1016/j.ecss.2020.107156.

Khawfany, A.A.; Aref, M.A.; Matsah, M.I. and Taj, R.J. (2017). Utilizing Landsat-8 data in mapping of sabkha, mangroves, and land covers in Jizan coastal plain, southwestern Saudi Arabia. Arab. J. Geosci., 10(5): 103 – 121 . https://doi.org/10.1007/s12517-017-2904-5.

Lovelock, C.E. and Reef, R. (2020). Variable Impacts of Climate Change on Blue Carbon. One Earth., 3(2): 195 – 211. https://doi.org/10.1016/j.oneear.2020.07.010.

Madkour, H.A.; Mansour, A.M.; Ahmed, A.E.H.N. and El-Taher, A. (2014). Environmental texture and geochemistry of the sediments of a subtropical mangrove ecosystem and surrounding areas, Red Sea Coast, Egypt. Arab. J. Geosci., 7(9): 3427 – 3440. https://doi.org/10.1007/s12517-013-0977-3.

Madkour, H.A. and Mohammed, A.W. (2008). Nature and geochemistry of surface sediments of the mangrove environment along the Egyptian Red Sea coast. Environ. Geol., 54(2): 257 – 267. https://doi.org/10.1007/s00254-007-0813-8.

McLeod, E.; Chmura, G.L.; Bouillon, S.; Salm, R.; Björk, M.; Duarte, C.M.; Lovelock, C.E.; Schlesinger, W.H. and Silliman, B.R. (2011). A blueprint for blue carbon: toward an improved understanding of the role of vegetated coastal habitats in sequestering CO2. Front. Ecol. Environ., 9(10): 552 – 560. https://doi.org/10.1890/110004.

Meersmans, J.; De Ridder, F.; Canters, F.; De Baets, S. and Van Molle, M. (2008). A multiple regression approach to assess the spatial distribution of Soil Organic Carbon (SOC) at the regional scale (Flanders, Belgium). Geoderma., 143(1): 11 – 13. https://doi.org/10.1016/j.geoderma.2007.08.025.

Nguyen, H.H.; Nghia, N.; Nguyen, H.; Le, A.; Tran, L.; Duong, L. and Böhm, S., Furniss, M.J. (2020). Classification Methods for Mapping Mangrove Extents and Drivers of Change in Thanh Hoa Province, Vietnam during 2005-2018. For. Soc., 4: 225 – 242. https://doi.org/10.24259/fs.v4i1.9295.

Perera, K.A.R.S. and Amarasinghe, M.D. (2019). Carbon sequestration capacity of mangrove soils in micro tidal estuaries and lagoons: A case study from Sri Lanka. Geoderma., 347: 80 – 89. https://doi.org/10.1016/j.geoderma.2019.03.041.

Polina, L. (2018). Sediment Particle Size Analysis: Report on Grain Size Experiment. College of Marine Geo-sciences, China.

Radabaugh, K.R.; Moyer, R.P.; Chappel, A.R.; Powell, C.E.; Bociu, I.; Clark, B.C. and Smoak, J.M. (2018). Coastal Blue Carbon Assessment of Mangroves, Salt Marshes, and Salt Barrens in Tampa Bay, Florida, USA. Estuaries Coast., 41(5): 1496 – 1510. https://doi.org/10.1007/s12237-017-0362-7.

Romañach, S.S.; DeAngelis, D.L.; Koh, H.L.; Li, Y.; Teh, S.Y.; Raja Barizan, R.S and Zhai, L. (2018.) Conservation and restoration of mangroves: Global status, perspectives, and prognosis. Ocean Coast Manag., 154: 72 – 82. https://doi.org/10.1016/j.ocecoaman.2018.01.009.

Rousel, J.; Haas, R.; Schell, J. and Deering, D. (1973). Monitoring vegetation systems in the Great Plains with ERTS. Third ERTS Symposium. NASA SP-351, Washington, D.C., pp. 309 – 317.

Saleh, M.A. (2007). Assessment of mangrove vegetation on Abu Minqar Island of the Red Sea. J. Arid Environ., 68(2): 331 – 336. https://doi.org/10.1016/j.jaridenv.2006.05.016.

Salem, B.B.; Andersen, G.L. and Zahran, M.A. (2008). Remote Sensing and Vegetation Map of Egypt, in: Zahran, M. A., Willis, A. J. (Eds.), The Vegetation of Egypt. Springer, London. pp. 319 – 333.

Shaltout, K.H.; Ahmed, M.T.; Alrumman, S.A.; Ahmed, D.A. and Eid, E.M. (2020). Evaluation of the carbon sequestration capacity of arid mangroves along nutrient availability and salinity gradients along the Red Sea coastline of Saudi Arabia. Oceanologia., 62(1): 56 – 69. https://doi.org/10.1016/j.oceano.2019.08.002.

Shaltout, K.H.; El-bana, M. and Said, P. (2019). Ecology of the Mangrove Forests along the Egyptian Red Sea Coast LAP Lambert Academic Publishing, Germany.

Taylor, M. and Stephenson, K. (2017). Impacts of climate change on sea temperature in the coastal and marine environments of Caribbean Small Island Developing States (SIDS). Clim. Change Rep. Card: Sci. Rev., 1994: 23 – 30.

Wang, L.; Jia, M.; Yin, D. and Tian, J. (2019). A review of remote sensing for mangrove forests: 1956–2018. Remote Sens. Environ., 231: 111223. https://doi.org/10.1016/j.rse.2019.111223.

Ward, R.D.; Friess, D.A.; Day, R.H. and MacKenzie, R.A. (2016). Impacts of climate change on mangrove ecosystems: a region by region overview. Ecosyt. Health Sust., 2(4): e01211. https://doi.org/10.1002/ehs2.1211.

Wilke, B.M. (2005). Determination of Chemical and Physical Soil Properties, in: Margesin, R., Schinner, F. (Eds.), Monitoring and Assessing Soil Bioremediation. Springer, Berlin, Heidelberg. pp. 47-95.

Xiaonan, D.; Xiaoke, W.; Lu, F. and Zhiyun, O. (2008). Primary evaluation of carbon sequestration potential of wetlands in China. Acta Ecologica Sinica., 28(2): 463 – 469. https://doi.org/10.1016/S1872-2032(08)60025-6.